Robocentric Mapping and Localization in Modified Spherical Coordinates with Bearing Measurements

Anders Boberg, Adrian N. Bishop and Patric Jensfelt

Centre for Autonomous Systems (CAS), Royal Institute of Technology (KTH)

aboberg@kth.se, adrian.bishop@ieee.org, patric@kth.se

***Abstract*—In this paper, a new approach to robotic mapping is presented that uses modified spherical coordinates in a robot-centered reference frame and a bearing-only measurement model. The algorithm provided in this paper permits robust delay-free state initialization and is computationally more efficient than the current standard in bearing-only (delay-free initialized) simultaneous localization and mapping (SLAM). Importantly, we provide a detailed nonlinear observability analysis which shows the system is generally observable. We also analyze the error convergence of the filter using stochastic stability analysis. We provide an explicit bound on the asymptotic mean state estimation error. A comparison of the performance of this filter is also made against a standard world-centric SLAM algorithm in a simulated environment.**

I. Introduction

Simultaneous localization and mapping (SLAM) is a well researched problem within robotics. Many implementations and scenario variations exist using a variety of different filters [1]–[4]. However, it is surprising that within the SLAM literature, there is relatively little research on the use of, and subsequent performance surrounding, different coordinate systems or on the analysis of the filter error convergence. In the closely related field of target tracking, research has shown that coordinate transforms that linearize the measurement model may improve error convergence [5], [6]. Indeed, in traditional target tracking [5] the system dynamic model is often originally linear in Cartesian coordinates. However, by changing coordinates in order to derive an analytically linear measurement model we typically sacrifice this linearity of the system model. Nevertheless, overall estimation performance is often improved as discussed in [5], [6]. In robotic mapping and localization algorithms we typically start with a nonlinear system model in any case. Moreover, in the typical world-centric SLAM formulation we start with an unobservable [7], [8] nonlinear (in both system and measurements) state estimation problem.

The unobservability of the world-centric SLAM problem [7], [8] suggests that a robot-centric formulation may be more appropriate. Moreover, estimator inconsistencies caused by accumulated linearization errors [9]–[11] are exasperated in world-centric coordinates, particularly for extended Kalman filter-like (EKF) algorithms. In [12] the concept of robocentric mapping is introduced and shown to better deal with linearization errors than the traditional SLAM formulation.

This work was supported by the Swedish Foundation for Strategic Research (SSF) through CAS and also via the EU FP7 project 'CogX'.

One contribution of this paper is an algorithm for robocentric bearings-only SLAM which uses a modified spherical coordinate system. The problem of bearing-only SLAM is of interest since many sensors are capable only of providing the bearing of target-points-of-interest. For example, single camera, vision-based, measurement systems provide only the bearings to particular points in three-dimensional space [13]. Similarly, passive sensing technology often provides only target bearing information. By building a map in a relative spherical-like framework, we eliminate the nonlinearities associated with the measurement equation. Moreover, we eliminate the problems associated with the unobservable states [7] and the inconsistencies caused by the EKF linearizations (which alter the unobservable subspace [7]).

Another important contribution of this paper is the inclusion of a rigorous observability analysis. We show that in general, our robocentric system state is observable, i.e. the relative location of the landmarks are observable, given only relative bearing measurements. We go further than this and provide conditions under which the state estimation error of an EKF-like algorithm is bounded. The convergence analysis in this paper is actually conservative, with the particular asymptotic properties of the mean estimation error dependent on the exact robot trajectory; e.g. see [14], [15]. The analysis in this paper is provided in order to justify the modified spherical coordinates considered, and the wide application of the EKF in mapping (and, in particular, in mapping in this coordinate framework).

The work in this paper differs from that in the target tracking literature since we consider a nonlinear robot dynamic model. We then rigorously analyze the observability and convergence of an EKF-like algorithm given the particular nonlinear dynamics, bearing-only measurements and the modified coordinate system. We differ from related work in the robot mapping and localization literature by introducing a new coordinate system, within which a number of distinct advantages are shown to exist. We also differ from existing robotic mapping papers by introducing a rigorous convergence and observability analysis for the estimation problem. This analysis will be of interest to roboticists employing similarly structured algorithms.

II. Preliminaries

We assume a robot moving on a planar surface according to the unicycle motion model. The robot state is described by the vector $\mathbf{x}_r = [x_r\ y_r\ z_r\ \phi_r]^{\mathrm{T}}$. The robot is steered using the inputs v_r and ω_r, which are the translational and angular velocities. The robot's motion is described by the following system of nonlinear equations

$$\begin{aligned} \dot{x}_r &= v_r \cos\phi_r \\ \dot{y}_r &= v_r \sin\phi_r \\ \dot{z}_r &= 0 \\ \dot{\phi}_r &= w_r \end{aligned} \tag{1}$$

These inputs are disturbed by the noise components v_n and ω_n, which are assumed to be uncorrelated zero-mean Weiner processes with standard deviations σ_v and σ_ω. The full stochastic motion model for the robot is described by

$$d\begin{bmatrix} x_r \\ y_r \\ z_r \\ \phi_r \end{bmatrix} = \begin{bmatrix} v_r\cos\phi_r \\ v_r \sin\phi_r \\ 0 \\ \omega_r \end{bmatrix} dt + \begin{bmatrix} \sigma_v \cos\phi_r & 0 \\ \sigma_v \sin\phi_r & 0 \\ 0 & 0 \\ 0 & \sigma_\omega \end{bmatrix} \begin{bmatrix} dv_n \\ d\omega_n \end{bmatrix} \tag{2}$$

The robot moves through an environment populated by n point landmarks, which it is capable of observing through bearing measurements. We denote by $\mathcal{V}$ the set of all such landmarks and by $\mathcal{G}(t) \subset \mathcal{V}$ the set of landmarks observable at time t. Let the Cartesian coordinates of the ith landmark be denoted by $\mathbf{p}_i = [x_i \; y_i \; z_i]^\top$. Then the true measurements of the ith landmark can be expressed as

$$\begin{aligned} \alpha_i &= \arctan\frac{y_i - y_r}{x_i - x_r} - \phi_r \\ \beta_i &= \arcsin\frac{z_i - z_r}{\sqrt{(x_i-x_r)^2 + (y_i-y_r)^2 + (z_i-z_r)^2}} \end{aligned} \tag{3}$$

or concisely using the measurement vector $\mathbf{y}_i(t) = [\alpha_i(t) \; \beta_i(t)]^\top$. Let $\mathbf{z} = [\mathbf{x}_r^\top \; \mathbf{p}_i^\top \; \ldots \; \mathbf{p}_n^\top]^\top$ denote a traditional SLAM state vector. The measurements $\mathbf{y}_i(t)$ are typically corrupted by a noise process $\mathbf{n}(t)$ such that

$$d\mathbf{y}(t) \triangleq \psi dt = h(\mathbf{z})dt + \mathbf{E}(t)\mathbf{n}(t) \tag{4}$$

in continuous-time. Here, we assume that $\mathbf{n}(t)$ is a zero-mean Weiner process and $\mathbf{E}(t)$ is a measurement noise weighting matrix that can be dependent on the true state. The measurements and robot dynamics are nonlinear in the chosen Cartesian coordinate system.

III. Robocentric Mapping in Modified Spherical Coordinates

The contribution of this paper is a novel robocentric algorithm for mapping and localization which takes advantage of the spherical-like nature of the relative bearing measurements. There does not appear to be any similar (spherical-like) algorithms in the SLAM or robocentric mapping literature.

The spherical coordinates of landmark i in the robot's reference frame is given by

$$\begin{aligned} \alpha_i &= \arctan\frac{y_i - y_r}{x_i - x_r} - \phi_r \\ \beta_i &= \arcsin\frac{z_i - z_r}{\sqrt{(x_i-x_r)^2 + (y_i-y_r)^2 + (z_i-z_r)^2}} \\ d_i &= \sqrt{(x_i-x_r)^2 + (y_i-x_r)^2 + (z_i-z_r)^2} \end{aligned} \tag{5}$$

which we write succinctly as $\mathbf{r}_i = [\alpha_i \; \beta_i \; d_i]^\top$. Using (5) together with the unicycle motion model (1) of the robot yields

$$\begin{aligned} \dot{\alpha}_i &= \frac{v_r \sin\alpha_i}{d_i \cos\beta_i} - \omega_r \\ \dot{\beta}_i &= \frac{v_r}{d_i}\cos\alpha_i \sin\beta_i \\ \dot{d}_i &= -v_r \cos\alpha_i \cos\beta_i \end{aligned} \tag{6}$$

Taking the previously defined noise processes v_n and ω_n into account, we get the following stochastic motion model

$$\begin{aligned} d\begin{bmatrix} \alpha_i \\ \beta_i \\ d_i \end{bmatrix} &= \begin{bmatrix} \frac{v_r \sin\alpha_i}{d_i\cos\beta_i} - \omega_r \\ \frac{v_r}{d_i}\cos\alpha_i \sin\beta_i \\ -v_r\cos\alpha_i\cos\beta_i \end{bmatrix} dt + \\ & \begin{bmatrix} \frac{\sigma_v \sin\alpha_i}{d_i\cos\beta_i} & -\sigma_\omega \\ \frac{\sigma_v}{d_i}\cos\alpha_i\sin\beta_i & 0 \\ -\sigma_v\cos\alpha_i\cos\beta_i & 0 \end{bmatrix} \begin{bmatrix} dv_n \\ d\omega_n \end{bmatrix} \end{aligned} \tag{7}$$

We thus have a nonlinear system (7) and linear measurements (9). However, we go one step further and modify the dynamic system (7) slightly. In particular, we will not consider the range d_i of each landmark i but rather the inverse range $\rho_i = 1/d_i$, see [5], [13]. In this case, we have $\dot{\rho}_i = -\rho_i^2 \dot{d}_i$ or taking account of the input noise we have

$$d\rho_i = v_r\rho_i^2 \cos\alpha_i \cos\beta_i dt + \sigma_v \rho_i^2 \cos\alpha_i \cos\beta_i dv_n \tag{8}$$

and thus the modification of the dynamic system (7) is obvious. The reason for using ρ_i instead of d_i is related to the initialization and is explained in the subsequent subsection. We redefine $\mathbf{r}_i = [\alpha_i \; \beta_i \; \rho_i]^\top$ and $\mathbf{z} = [\mathbf{r}_1 \; \ldots \; \mathbf{r}_n]^\top$. The measurements (3) are linear in $\mathbf{r}_i$ or more generally in $\mathbf{z} = [\mathbf{r}_1 \; \ldots \; \mathbf{r}_n]^\top$ and can then be given by the continuous-time measurement equation

$$d\mathbf{y}(t) \triangleq \psi dt = \mathbf{H}(\mathcal{G}(t))\mathbf{z}dt + \mathbf{E}(t)\mathbf{n}(t) \tag{9}$$

where $\mathbf{E}(t)$ is not required to be independent of $\mathbf{z}$. Here, $\mathbf{H}(\mathcal{G}(t))$ is a time-varying linear matrix which is dependent only on the set $\mathcal{G}(t)$ of currently sensed landmarks.

The function $f_i(\cdot)$ which captures the dynamics of the subspace $\mathbf{r}_i$ is

$$f_i(\widehat{\mathbf{z}}, v_r, w_r) = f_i(\widehat{\mathbf{r}}_i, v_r, w_r) = \begin{bmatrix} \frac{v_r\rho_i \sin\alpha_i}{\cos\beta_i} - \omega_r \\ v_r\rho_i\cos\alpha_i\sin\beta_i \\ v_r\rho_i^2\cos\alpha_i\cos\beta_i \end{bmatrix} \tag{10}$$

and where $f(\cdot)$ is thus a vertical concatenation of the $f_i(\cdot)$. For latter use we introduce the following Taylor expansion of $f(\cdot)$ about the estimate $\widehat{\mathbf{z}}$,

$$f(\mathbf{z}, v_r, w_r) - f(\widehat{\mathbf{z}}, v_r, w_r) = \mathbf{A}(t)(\mathbf{z} - \widehat{\mathbf{z}}) + \varrho(\mathbf{z}, \widehat{\mathbf{z}}, v_r, w_r) \tag{11}$$

where $\mathbf{A}(t)$ is the Jacobian of $f(\cdot)$ and $\varrho(\mathbf{z}, \widehat{\mathbf{z}}, v_r, w_r)$ accounts for the higher order terms. The Jacobian $\mathbf{A}_i(t)$ of $f_i(\cdot)$ is given by

$$\mathbf{A}_i = v_r\rho_i^2 \begin{bmatrix} \frac{\cos\alpha_i}{\rho_i\cos\beta_i} & \frac{\sin\alpha_i\sin\beta_i}{\rho_i\cos^2\beta_i} & \frac{\sin\alpha_i}{\rho_i^2\cos\beta_i} \\ -\frac{\sin\alpha_i\sin\beta_i}{\rho_i} & \frac{\cos\alpha_i\cos\beta_i}{\rho_i} & \frac{\cos\alpha_i\sin\beta_i}{\rho_i^2} \\ -\sin\alpha_i\cos\beta_i & -\cos\alpha_i\sin\beta_i & \frac{2\cos\alpha_i\cos\beta_i}{\rho_i} \end{bmatrix} \tag{12}$$

and is evaluated at an estimate $\widehat{\mathbf{r}_i}$. For any time-varying matrix $\mathbf{M}(t)$ we introduce the following notation

$$\|\mathbf{M}(t)\| = \sup\{\|\mathbf{M}(t)\| : m_{ij} \in \mathbb{R}\} \tag{13}$$

for all t and for some norm $\|\cdot\|$. Moreover, we make the following standing assumption for simplicity.

Assumption 1: The robot does not travel directly over or directly underneath a true landmark location or the estimated location of a landmark, i.e. $\beta_i \neq \pm\pi/2$ *or* $\widehat{\beta}_i \neq \pm\pi/2$.

Assumption 1 is a technical requirement of the chosen coordinate system but not strong in practice. In fact, landmarks are often not chosen automatically to lie directly above or below the robot's trajectory and if indeed they were then we could subsequently alter the robot trajectory to avoid this. As a consequence of the assumption, the following bound holds

$$\|\mathbf{A}(t)\| = \overline{a} < \infty \tag{14}$$

for all t given a particular robot trajectory. The error $\zeta = \mathbf{z} - \widehat{\mathbf{z}}$ is the so-called state estimation error. We will also need the following lemma concerning the growth of $\varrho(\mathbf{z}, \widehat{\mathbf{z}}, v_r, w_r)$.

Lemma 1: The following inequality holds

$$\begin{aligned} \|\varrho(\mathbf{z}, \widehat{\mathbf{z}}, v_r, w_r)\| &= \|f(\mathbf{z}, \cdot) - f(\widehat{\mathbf{z}}, \cdot) - \mathbf{A}(t)(\mathbf{z} - \widehat{\mathbf{z}})\| \\ &\leq 2\overline{a}\|\zeta\| \end{aligned} \tag{15}$$

for with probability 1 *when Assumption 1 holds.*

Proof: From the triangle inequality we obtain

$$\begin{aligned} \|f(\mathbf{z}, v_r, w_r) - f(\widehat{\mathbf{z}}, v_r, w_r) - \mathbf{A}(t)(\mathbf{z} - \widehat{\mathbf{z}})\| &\leq \\ \|f(\mathbf{z}, v_r, w_r) - f(\widehat{\mathbf{z}}, v_r, w_r)\| + \| - \mathbf{A}(t)\zeta\| &\leq \\ \|f(\mathbf{z}, v_r, w_r) - f(\widehat{\mathbf{z}}, v_r, w_r)\| + \overline{a}\zeta & \end{aligned} \tag{16}$$

which follows using (14). Now if $f(\cdot)$ is Lipschitz then $\|f(\mathbf{z}, v_r, w_r) - f(\widehat{\mathbf{z}}, v_r, w_r)\| \leq c\|\mathbf{z} - \widehat{\mathbf{z}}\|$ for some $0 < c < \infty$. Actually, we know that if $\|\mathbf{A}(t)\|$ is bounded by $\overline{a}$ then $f(\cdot)$ is Lipschitz with Lipschitz coefficient $\overline{a}$. ■

Note also that $\varrho(\mathbf{z}, \widehat{\mathbf{z}}, v_r, w_r) = 0$ when $\zeta(t) = 0$.

A. Initialization in Modified Spherical Coordinates

Since the location of the landmarks, or even their number, is not known beforehand, we will need to augment our state with the parameters for each new landmark when they are first observed. This presents a problem, since we only observe the two bearings, α and β, in any single measurement, and not the depth (or inverse depth).

This problem is particularly severe in Cartesian coordinates, since the conic region of uncertainty will not be well approximated by a Gaussian distribution. One way to get around this is to use so called *delayed initialization* [16], where a landmark is not added to the state until it has been observed sufficiently for the depth to be estimated. However, this adds to the complexity of the implementation, requiring the provisional landmarks to be handled as a separate case.

Civera et al. [13] proposed a method for undelayed initialization for global SLAM by parameterizing the landmarks using the robot pose in Cartesian coordinates together with the two observed bearings and the inverse depth. In our robocentric formulation, we will only use the latter three parameters. The bearings are trivially initialized using the measurement values and measurement statistics. The uncertainty in the inverse depth can be reasonably well approximated using a Gaussian function [13]. Also, by using the inverse depth ρ_i instead of d_i, we can better account for a very large range of initial d_i values (including ∞) in the uncertainty region given a reasonable value for $\rho_i(0)$ and $\sigma_\rho(0)$.

B. Observability of the Proposed Estimation Problem

When discussing the observability of the proposed SLAM algorithm, we will use the property of *local weak observability*, as defined by Hermann and Krener in [17]. The same method was previously applied to the global SLAM problem in [8] to prove its fundamental unobservability.

A system Σ is said to be *locally weakly observable* at a point $\mathbf{x}^0$ if we can instantaneously distinguish $\mathbf{x}^0$ from its neighbors. To test for this property, we use the *observability rank condition*, which is a sufficient condition for local weak observability. For simplicity, we will only consider a system with a single landmark i. We define our system Σ as

$$\Sigma: \begin{array}{l} \dot{\mathbf{x}} = f(\mathbf{x}, v_r, \omega_r) = \begin{pmatrix} f_\alpha \\ f_\beta \\ f_\rho \end{pmatrix} = \begin{pmatrix} \frac{v_r \rho_i \sin\alpha_i}{\cos\beta_i} - \omega_r \\ v_r \rho_i \cos\alpha_i \sin\beta_i \\ v_r \rho_i^2 \cos\alpha_i \cos\beta_i \end{pmatrix} \\ \mathbf{y} = h(\mathbf{x}) = \begin{pmatrix} h_1 \\ h_2 \end{pmatrix} = \begin{pmatrix} \alpha_i \\ \beta_i \end{pmatrix} \end{array}$$

where $\mathbf{x} \in \mathcal{M}$ and $\mathcal{M}$ is a 3-dimensional C^∞ connected manifold and f and h are C^∞ functions.

Let O_Σ be the matrix whose rows consist of repeated Lie derivatives of one-forms $dh_i(\mathbf{x})$ with respect to the Lie algebra $\mathcal{F}$ of vector fields generated by $f(\mathbf{x}, v_r, \omega_r)$ on $\mathcal{M}$. These repeated Lie derivatives are defined recursively as

$$L_f^0 dh_i(\mathbf{x}) = \frac{\partial h_i(\mathbf{x})}{\partial \mathbf{x}} \tag{17}$$

and given an iterative index $q \in \mathbb{N}$ we have

$$\begin{aligned} L_f^q dh_i(\mathbf{x}) &= L_f^{q-1} dh_i(\mathbf{x}) \frac{\partial f(\mathbf{x}, v_r, \omega_r)}{\partial \mathbf{x}} \\ &\quad + \left[\frac{\partial}{\partial \mathbf{x}} \left(L_f^{D-1} dh_i(\mathbf{x}) \right)^{\mathrm{T}} f(\mathbf{x}, v_r, \omega_r) \right]^{\mathrm{T}} \end{aligned} \tag{18}$$

For our system Σ, we have

$$L_f^0 dh_1 = [1\ 0\ 0], \qquad L_f^0 dh_2 = [0\ 1\ 0] \tag{19}$$

$$L_f^1 dh_1 = v_r \left[\frac{\rho_i \cos\alpha_i}{\cos\beta_i} \ \ \frac{\rho_i \sin\alpha_i \sin\beta_i}{\cos^2\beta_i} \ \ \frac{\sin\alpha_i}{\cos\beta_i} \right] \tag{20}$$

$$L_f^1 dh_2 = v_r \rho_i [\frac{-\sin\alpha_i \sin\beta_i}{v_r} \ \ \cos\alpha_i \cos\beta_i \ \ \cos\alpha_i \sin\beta_i] \tag{21}$$

$$L_f^2 dh_1(\mathbf{x}) = \begin{bmatrix} \frac{4 v_r^2 \rho_i^2 \cos^2\alpha_i}{\cos^2\beta_i} - \frac{2 v_r^2 \rho_i^2}{\cos^2\beta_i} + \frac{v_r \omega_r \rho_i \sin\alpha_i}{\cos\beta_i} \\ \frac{4 v_r^2 \rho_i^2 \sin\alpha_i \cos\alpha_i \sin\beta_i}{\cos^2\beta_i} - \frac{v_r \omega_r \rho_i \cos\alpha_i \sin\beta_i}{\cos\beta_i} \\ \frac{4 v_r^2 \rho_i \sin\alpha_i \cos\alpha_i}{\cos^2\beta_i} - \frac{v_r \omega_r \cos\alpha_i}{\cos\beta_i} \end{bmatrix}^\top \tag{22}$$

$$L_f^2 dh_2(\mathbf{x}) = \begin{bmatrix} \frac{2v_r^2\rho_i^2 \sin\alpha_i \cos\alpha_i \sin\beta_i}{\cos\beta_i} - 4v_r^2\rho_i^2 \sin\alpha_i \cos\alpha_i \sin\beta_i \cos\beta_i + v_r\omega_i\rho_i \cos\alpha_i \sin\beta_i \\ 4v_r^2\rho_i^2 \cos^2\alpha_i \cos^2\beta_i - 2v_r^2\rho_i^2 \cos^2\alpha_i - \frac{v_r^2\rho_i^2 \sin^2\alpha_i}{\cos^2\beta_i} + v_r\omega_r \cos\alpha_i \sin\beta_i \\ 4v_r^2\rho_i \cos^2\alpha_i \sin\beta_i \cos\beta_i - \frac{2v_r^2\rho_i \sin^2\alpha_i \sin\beta_i}{\cos\beta_i} + v_r\omega_r \sin\alpha_i \sin\beta_i \end{bmatrix}^\top \tag{23}$$

If $\mathrm{rank}(\mathrm{O}_\Sigma) = 3$, for some point $\mathbf{x}^0$, the system fulfills the observability rank condition at this point, and is thus locally weakly observable at this point [17].

Note by inspection, if $v_r = 0$, O_Σ will never be full rank since the third column will be zero. Intuitively, the robot is stationary and can never observe any change in the landmark bearings and thus cannot observe depth. If $v_r \neq 0$ and $\omega_r = 0$ then (20) and (21) ensure that the observability rank condition will hold as long as α_i and β_i are not both equal to zero. This means that Σ will be locally weakly observable for all $\mathbf{x}$ with $\alpha_i \neq 0$ and $\beta_i \neq 0$. This also agrees with intuition, since if the robot was moving directly towards the landmark, it would not observe any change in bearing.

Finally, if both $v_r \neq 0$ and $\omega_r \neq 0$ then (22) ensures that the observability rank condition will hold for every $\mathbf{x} \in \mathcal{M}$ and thus Σ will be locally weakly observable. Intuitively, this corresponds to the robot traveling on an arc, so that no landmark will remain on the indistinguishable line.

C. The Estimator

The behavior of an estimate $\widehat{\mathbf{z}}$ of $\mathbf{z}$ depends on the particular estimator. Thus we consider an estimator of the form

$$d\widehat{\mathbf{z}} = f(\widehat{\mathbf{z}}, v_r, w_r)dt + \mathbf{K}(t)\left(d\mathbf{y}(t) - \mathbf{H}(\mathcal{G}(t))\widehat{\mathbf{z}}dt\right) \tag{24}$$

The gain $\mathbf{K}(t)$ is given by

$$\mathbf{K}(t) = \mathbf{P}(t)\mathbf{H}^\top(\mathcal{G}(t))\mathbf{R}^{-1}(t) \tag{25}$$

and $\mathbf{P}(t)$ is the solution to the following Riccati differential equation

$$\begin{aligned} d\mathbf{P}(t) &= \left[\mathbf{A}(t)\mathbf{P}(t) + \mathbf{P}(t)\mathbf{A}^\top(t) + \mathbf{Q}(t)\right]dt - \\ &\quad \mathbf{P}(t)\mathbf{H}^\top(\mathcal{G}(t))\mathbf{R}^{-1}(t)\mathbf{H}(\mathcal{G}(t))\mathbf{P}(t) \end{aligned} \tag{26}$$

where $\mathbf{Q}$ and $\mathbf{R}$ are positive-definite tuning matrices. For completeness we state the following common assumption.

Assumption 2: The following $\mathbf{Q}(t) \geq \underline{q}\mathbf{I}$, $\mathbf{R}(t) \geq \underline{r}\mathbf{I}$ and $\mathbf{P}(t_0) \geq p_0\mathbf{I}$ are given for some $\underline{q}, \underline{r}, p_0 > 0$ such that $\|\mathbf{Q}(t)\| \geq \underline{q}$ and $\|\mathbf{R}(t)\| \geq \underline{r}$. Moreover, $\mathbf{Q}(t)$ and $\mathbf{R}(t)$ are chosen to be bounded by $\|\mathbf{Q}(t)\| \leq \overline{q} < \infty$ and $\|\mathbf{R}(t)\| \leq \overline{r} < \infty$ for all t. Also, we have $\mathbf{E}(t) \leq \overline{e} < \infty$ with $\mathbf{E}(t) \geq \underline{e}\mathbf{I}$.

The analysis in this paper will consider the propagation of the estimation error $\zeta(t) = \mathbf{z}(t) - \widehat{\mathbf{z}}(t)$ for all $t > t_0$ given an initial estimation error $\zeta(t_0)$ which we will assume belongs to the set

$$\|\zeta(t_0)\| \leq b \quad \text{in the state space} \tag{27}$$

for some constant $b < \infty$. We assume initially that $\widetilde{\mathcal{G}}(t) = \mathcal{G}$ for all $t > t_0$. It is common to assume a full landmark measurement vector for analysis [3], [11].

Note that in general, the continuous time estimator in this section does not involve a prediction stage. However, by letting $\mathbf{R}^{-1}(t) = 0$ over the time interval $t \in [k_0, k_1]$ we can easily allow for the absence of measurements over that interval.

D. On the Convergence of the Feature Estimator

We consider (for simplicity) the case where $\tilde{\mathcal{G}}(t) = \mathcal{G}(t)$ for all t. We assume an EKF-like algorithm of the form (24) with Assumptions 1-2 holding. The error $\zeta = \mathbf{z} - \widehat{\mathbf{z}}$ obeys

$$\begin{aligned} d\zeta &= \left[(\mathbf{A}(t) - \mathbf{K}(t))\,\zeta + \varrho(\mathbf{z}, \widehat{\mathbf{z}}, v_r, w_r)\right]dt + \\ &\quad \mathbf{G}(t)\begin{bmatrix} dv_n \\ dw_n \end{bmatrix} - \mathbf{K}(t)\mathbf{E}(t)d\mathbf{n}(t) \\ d\zeta &= \left[(\mathbf{A}(t) - \mathbf{K}(t))\,\zeta + \varrho(\mathbf{z}, \widehat{\mathbf{z}}, v_r, w_r)\right]dt + \\ &\quad \left[\mathbf{G}(t) \;\; -\mathbf{K}(t)\mathbf{E}(t)\right]\begin{bmatrix} \begin{bmatrix} dv_n \\ dw_n \end{bmatrix} \\ d\mathbf{n}(t) \end{bmatrix} \end{aligned} \tag{28}$$

where $\mathbf{G}_i(t)$ is given by

$$\|\mathbf{G}_i(t)\| = \left\| \begin{bmatrix} \frac{\sigma_v\rho_i \sin\alpha_i}{\cos\beta_i} & -\sigma_\omega \\ \rho_i\sigma_v \cos\alpha_i \sin\beta_i & 0 \\ -\sigma_v\rho_i^2 \cos\alpha_i \cos\beta_i & 0 \end{bmatrix} \right\| = \overline{g} < \infty \tag{29}$$

and $\mathbf{G}(t) = \begin{bmatrix}\mathbf{G}_1^\top & \dots & \mathbf{G}_n^\top\end{bmatrix}^\top$. Recall Lemma 1 bounds the growth of the nonlinear perturbation term $\varrho(\mathbf{z}, \widehat{\mathbf{z}}, v_r, w_r)$. We need the following assumption.

Assumption 3: The state covariance $\mathbf{P}(t)$ is bounded by

$$0 < \underline{p} \leq \mathbf{P}(t) \leq \overline{p} < \infty \tag{30}$$

for all $t > t_0$

Note that Assumption 3 is quite reasonable. In fact, the lower bound follows from a general controllability argument. We also conjecture based on the analysis in [18] that it is possible to formally prove that Assumption 3 holds for all t, given only that the control inputs ensure the state is observable, e.g. $v_r \neq 0$ for all t, and $\|\mathbf{A}(t)\|$ is bounded.

Theorem 1: Consider (28) with an initial condition (27) and $\mathcal{G}(t) = \mathcal{V}(t)$ for all t. Suppose that Assumptions 1-3 hold. If

$$\|\mathbf{P}^{-1}(t)\mathbf{Q}(t)\mathbf{P}^{-1}(t) + \mathbf{R}^{-1}(t)\|\underline{p} > 4\overline{ap}/\underline{p} \tag{31}$$

then the estimation error is bounded above with

$$\mathcal{E}\left\{\|\zeta(t)\|^2\right\} \leq \max\left\{\frac{n(\underline{r}^2\overline{g}^2 + \overline{p}\underline{p}\overline{e}^2)}{2\gamma\underline{r}^2\underline{p}},\ \frac{\overline{p}}{\underline{p}}\|\zeta(t_0)\|^2\right\} \tag{32}$$

where

$$\gamma = \|\mathbf{P}^{-1}(t)\mathbf{Q}(t)\mathbf{P}^{-1}(t) + \mathbf{R}^{-1}(t)\|\underline{p} - \frac{4\overline{ap}}{\underline{p}} \tag{33}$$

and $\mathcal{E}\left\{\|\zeta(t)\|^2\right\}$ as $t \to \infty$ is bounded by $\frac{n(\underline{r}^2\overline{g}^2 + \overline{p}\underline{p}\overline{e}^2)}{2\gamma\underline{r}^2\underline{p}}$.

Proof: Let $\mathcal{B}(t,\zeta(t)) = \zeta^\top(t)\mathbf{P}^{-1}(t)\zeta(t) > 0$ and note that

$$\begin{aligned} d\mathcal{B} &= \left[\frac{\partial\mathcal{B}}{\partial t} + \frac{\partial\mathcal{B}}{\partial\zeta}\left(\mathbf{A}(t) - \mathbf{K}(t)\right)\zeta + \frac{\partial\mathcal{B}}{\partial\zeta}\varrho(\mathbf{z},\widehat{\mathbf{z}},\cdot)\right]dt + \\ & \frac{1}{2}\mathrm{tr}\left(\mathrm{hess}(\mathcal{B})\mathbf{\Xi}(t)\mathbf{\Xi}^\top(t)\right)dt - \\ & \frac{\partial\mathcal{B}}{\partial\zeta}\mathbf{\Xi}(t)\left[\begin{array}{c}\left[\begin{array}{c} dv_n \\ dw_n\end{array}\right] \\ d\mathbf{n}(t)\end{array}\right] \end{aligned} \quad (34)$$

where $\mathbf{\Xi}(t) = [\mathbf{G}(t) \ \ -\mathbf{K}(t)\mathbf{E}(t)]$ and where we have employed Itos differential formula. Evaluating the terms and rearranging leads to

$$\begin{aligned} d\mathcal{B} &= \left[\zeta^\top\left[\mathbf{P}^{-1}(t)\mathbf{Q}(t)\mathbf{P}^{-1}(t) + \mathbf{R}^{-1}(t)\right]\zeta\right]dt + \\ & 2\zeta^\top\mathbf{P}^{-1}(t)\varrho(\mathbf{z},\widehat{\mathbf{z}},v_r,w_r)dt + \\ & \frac{1}{2}\mathrm{tr}\left(\mathbf{P}^{-1}(t)\mathbf{G}(t)\mathbf{G}^\top(t)\right)dt + \\ & \frac{1}{2}\mathrm{tr}\left(\mathbf{P}^{-1}(t)\mathbf{K}(t)\mathbf{K}^\top(t)\right)dt - \\ & 2\zeta^\top\mathbf{P}^{-1}(t)\mathbf{\Xi}(t)\left[\begin{array}{c}\left[\begin{array}{c} dv_n \\ dw_n\end{array}\right] \\ d\mathbf{n}(t)\end{array}\right] \\ \leq & \left[-\alpha\|\zeta\|^2 + \frac{4\overline{a}}{\underline{p}}\|\zeta\|^2 + \frac{n(\underline{r}^2\overline{g}^2 + \overline{p}\underline{p}\overline{e}^2)}{2\gamma\underline{r}^2\underline{p}}\right]dt - \\ & 2\zeta^\top\mathbf{P}^{-1}(t)\mathbf{\Xi}(t)\left[\begin{array}{c}\left[\begin{array}{c} dv_n \\ dw_n\end{array}\right] \\ d\mathbf{n}(t)\end{array}\right] \end{aligned} \quad (35)$$

where we have explicitly employed Lemma 1 and where

$$\alpha = \|\mathbf{P}^{-1}(t)\mathbf{Q}(t)\mathbf{P}^{-1}(t) + \mathbf{R}^{-1}(t)\| \quad (36)$$

Now noting that $\overline{p}^{-1}\|\zeta\|^2 \leq \mathcal{B}(t,\zeta(t)) \leq \underline{p}^{-1}\|\zeta\|^2$ and using the Bellman-Gromwall lemma [19] we come to

$$\begin{aligned} \mathcal{B}(t,\zeta(t)) \leq & \ \mathcal{B}(t_0,\zeta(t_0))\exp\left(-\gamma(t-t_0)\right) - \\ & 2\int_{t_0}^{t}\zeta^\top(\tau)\mathbf{P}^{-1}(\tau)\mathbf{\Xi}(\tau)\left[\begin{array}{c}\left[\begin{array}{c} dv_n(\tau) \\ dw_n(\tau)\end{array}\right] \\ d\mathbf{n}(\tau)\end{array}\right] + \\ & \frac{n(\underline{r}^2\overline{g}^2 + \overline{p}\underline{p}\overline{e}^2)}{2\gamma\underline{r}^2\underline{p}} - \\ & \frac{n(\underline{r}^2\overline{g}^2 + \overline{p}\underline{p}\overline{e}^2)}{2\gamma\underline{r}^2\underline{p}}\exp\left(-\gamma(t-t_0)\right) \end{aligned} \quad (37)$$

where $\gamma = \left(\alpha\underline{p} - 4\frac{\overline{a}\overline{p}}{\underline{p}}\right)$ with $\gamma > 0$ if and only if $\alpha\underline{p} > \frac{4\overline{a}\overline{p}}{\underline{p}}$. Taking the expectation of (49) and rearranging gives

$$\mathcal{E}\left\{\|\zeta(t)\|^2\right\} \leq \max\left\{\frac{n(\underline{r}^2\overline{g}^2 + \overline{p}\underline{p}\overline{e}^2)}{2\gamma\underline{r}^2\underline{p}},\ \frac{\overline{p}}{\underline{p}}\|\zeta(t_0)\|^2\right\} \quad (38)$$

for all t if $\gamma > 0$. The error $\mathcal{E}\left\{\|\zeta(t)\|^2\right\}$ as $t \to \infty$ is bounded by $\frac{n(\underline{r}^2\overline{g}^2 + \overline{p}\underline{p}\overline{e}^2)}{2\gamma\underline{r}^2\underline{p}}$. This completes the proof. ■

Importantly, we have provided conditions under which an EKF-like algorithm will yield an exponentially bounded and converging mean-square estimation error.

IV. Numerical Analysis

The proposed algorithm is now illustrated via simulation. We compare the performance of the spherical robot-centric SLAM algorithm against a global SLAM algorithm similar to the one used in [13] in a simulated environment.

The state of the global SLAM algorithm takes the form $\mathbf{g} = [x_r\ y_r\ z_r\ \phi_r\ \mathbf{b}_1^\top\ \ldots\ \mathbf{b}_n^\top]^\top$ with $\mathbf{b}_i = [x_{ir}^*\ y_{ir}^*\ z_{ir}^*\ \alpha_i^*\ \beta_i^*\ \rho_i^*]^\top$ for a single landmark i. The x_{ir}^*, y_{ir}^* and z_{ir}^* state components are the position of the robot in global coordinates when the landmark i is first initialized (or observed). Here α_i^*, β_i^* and ρ_i^* are the α_i, β_i and ρ_i values relative to the robot's position when landmark i is first initialized, i.e. $[x_{ir}^*\ y_{ir}^*\ z_{ir}^*]^\top$ and the position of landmark i. The reason for this parametrization [13] is that it enables us to do single step initialization of the landmarks, which would be very difficult using a purely Cartesian representation.

A typical map and robot trajectory is shown in Fig 1. In each simulation run, the landmarks are distributed randomly in a square pattern along the x and y axes, and uniformly on the z-axis. The robot moves along a randomly generated path in the center of the environment.

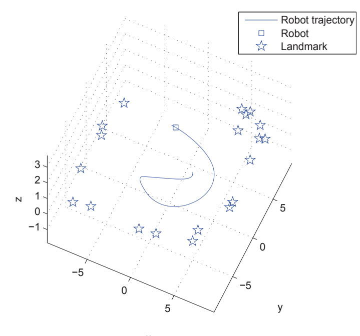

Fig. 1. A typical map layout and robot trajectory.

A. Example Scenario

In this case, the robot can sense landmark i if and only if $\alpha_i(t) \in (-\pi/4, \pi/4)$ and $\beta_i(t) \in (-\pi/4, \pi/4)$. The process noise is $\sigma_v = 0.42$, $\sigma_\omega = 1.06$ and the measurement noise has standard deviation 0.0873 radians for both bearings. Each simulation runs for 1500 time steps.

Since the robocentric algorithm does not estimate the robot's global position, we cannot compare the trajectories produced by the two algorithms. Thus, for the global algorithm, we generate a relative map by computing the estimated spherical landmark position relative to the estimated robot pose. The RMS errors are shown in Fig 2 over 1000 simulations. For both algorithms, the errors converge to a steady value and both perform well in terms of the relative map.

Note that Fig 2 does not illustrate the error in the robot pose or its effect on the global map. In some simulations, both the global map and the pose estimate were offset by a significant amount. Fig 3 shows a birds-eye view of such a case and highlights the flaws of world-centric mapping.

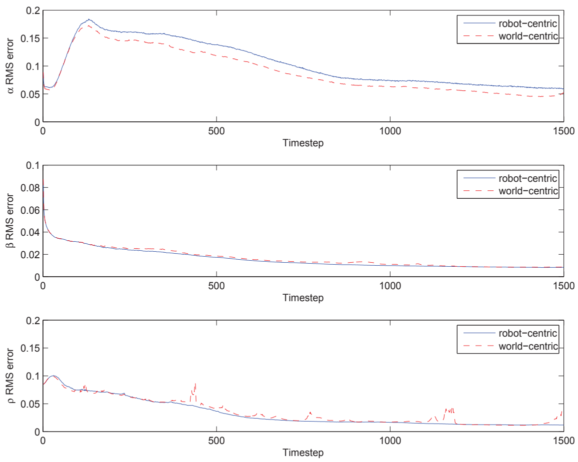

Fig. 2. The RMS error for the relative α bearings, β bearings and inverse distance ρ respectively.

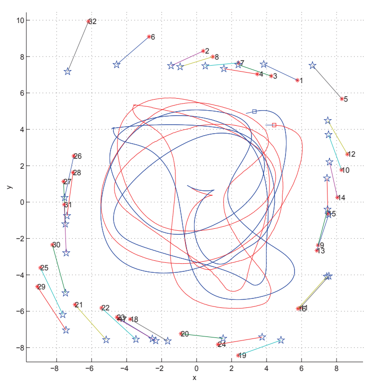

Fig. 3. This figure shows the global SLAM map and estimated robot trajectory is rotated and displaced quite significantly. The error in the global coordinates occurs despite, as shown in Fig 2, the fact that an accurate relative map can be derived from the global state.

This distortion of the global map is caused by an unobservable state in global SLAM, as was shown in [8].

V. A Note on Complexity

When analyzing the computational complexity of a SLAM algorithm, one critical factor is the size of the state. One of the costliest operations in the EKF is the multiplication of large matrices, which is typically $\mathcal{O}(m^3)$ for m-by-m matrices.

This gives the spherical robot-centric algorithm a significant speed boost over the global SLAM algorithm, since the size of the state is effectively cut in half. This speed boost was also notably observed in every simulation.

VI. Concluding Remarks

In this paper we proposed a computationally efficient robocentric mapping algorithm that can be implemented using a linear measurement equation. We further highlighted the problems caused by the unobservable state components in traditional, world-centric SLAM, i.e. Fig 3. We have illustrated (and suspect it is well known) that a relative map computed using the global SLAM state vector can perform comparably with a dedicated robocentric algorithm even if the actual global map is quite inaccurate. Given that only the relative state components are observable and the increased computational cost in maintaining a global map, we question the utility in doing so, and thus further motivate the work in this paper.

References

[1] R. Smith, M. Self, and P. Cheeseman, "Estimating uncertain spatial relationships in robotics," *Autonomous Robot Vehicles*, pp. 167–193, Springer-Verlag 1990.

[2] S. Thrun, D. Fox, and W. Burgard, "A probabilistic approach to concurrent mapping and localization for mobile robots," *Mach. Learning Autonom. Robots*, vol. 31, pp. 29–53, 1998.

[3] M. Dissanayake, P. Newman, S. Clark, H. Durrant-Whyte, and M. Csorba, "A solution to the simultaneous localization and map building (SLAM) problem," *IEEE Transactions on Robotics and Automation*, vol. 17, no. 3, pp. 229–241, June 2001.

[4] M. Walter, R. Eustice, and J. Leonard, "Exactly sparse extended information filters for feature-based SLAM," *International Journal of Robotics Research*, vol. 26, no. 4, pp. 335–359, April 2007.

[5] V. Aidala and S. Hammel, "Utilization of modified polar coordinates for bearings-only tracking," *IEEE Transactions on Automatic Control*, vol. 28, no. 3, p. 283294, March 1983.

[6] T. Song and J. Speyer, "A stochastic analysis of a modified gain extended Kalman filter with applications to estimation with bearings only measurements," *IEEE Transactions on Automatic Control*, vol. 30, no. 10, p. 940949, October 1985.

[7] G. Huang, A. Mourikis, and S. Roumeliotis, "Analysis and improvement of the consistency of extended Kalman filter based SLAM," in *Proceedings of the 2008 International Conference on Robotics and Automation (ICRA)*, May 2008, pp. 473–479.

[8] K. W. Lee, W. Wijesoma, and I. Javier, "On the observability and observability analysis of SLAM," in *2006 IEEE/RSJ International Conference on Intelligent Robots and Systems*, Oct. 2006, pp. 3569–3574.

[9] S. Julier and J. Uhlmann, "A counter example to the theory of simultaneous localization and map building," in *Proceedings of the 2001 International Conference on Robotics and Automation (ICRA)*, May 2001, pp. 4238–4243.

[10] T. Bailey, J. Nieto, J. Guivant, M. Stevens, and E. Nebot, "Consistency of the EKF-SLAM algorithm," in *Proceedings of the 2006 IEEE/RSJ International Conference on Intelligent Robots and Systems (IROS)*, October 2006, p. 35623568.

[11] S. Huang and G. Dissanayake, "Convergence and consistency analysis for extended kalman filter based SLAM," *IEEE Transactions on Robotics*, vol. 23, no. 5, pp. 1036–1049, October 2007.

[12] J. Castellanos, R. Martinez-Cantin, J. Tardos, and J. Neira, "Robocentric map joining: Improving the consistency of EKF-SLAM," *Robotics and Autonomous Systems*, vol. 55, no. 1, pp. 21–29, January 2007.

[13] J. Civera, A. Davison, and J. Montiel, "Inverse depth parametrization for monocular SLAM," *IEEE Transactions on Robotics*, vol. 24, no. 5, pp. 932–945, Oct. 2008.

[14] B. Grocholsky, J. Keller, V. Kumar, and G. Pappas, "Cooperative air and ground surveillance," *IEEE Robotics & Automation Magazine*, vol. 13, no. 3, pp. 16–25, September 2006.

[15] A. Bishop, B. Fidan, B. Anderson, K. Dogancay, and P. Pathirana, "Optimality analysis of sensor-target geometries in passive localization: Part 1 - Bearing-only localization," in *Proceedings of the 3rd International Conference on Intelligent Sensors, Sensor Networks and Information Processing (ISSNIP)*, December 2007.

[16] T. Bailey, "Constrained initialisation for bearing-only SLAM," in *Proceedings of the IEEE International Conference on Robotics and Automation (ICRA'03)*, September 2003, pp. 1966–1971.

[17] R. Hermann and A. Krener, "Nonlinear controllability and observability," *IEEE Transactions on Automatic Control*, vol. Ac-22, pp. 728–740, October 1977.

[18] A. Bishop and P. Jensfelt, "A stochastically stable solution to the problem of robocentric mapping," in *Proc. of ICRA'09*, Kobe, Japan, 2009.

[19] S. Sastry, *Nonlinear Systems: Analysis, Stability and Control.* New York, N.Y.: Springer-Verlag, 1999.